GMR
The Original

SYSTEMS PHARMACOLOGY AND MOLECULAR DOCKING UNCOVER THE MULTI-TARGET ANTICANCER LANDSCAPE OF *SPHAGNETICOLA CALENDULACEA* AGAINST OSTEOSARCOMA OF THE URINARY BLADDER

Aswathi K Biju[1], Sujitha Jesu Willson Ravi[2], K Hema Shree*[3], Parameswari R P[4]

[1]Department of Bioinformatics, Saveetha Medical College and Hospital, Saveetha Institute of Medical and Technical Sciences, Chennai-602105, India. Email: aswathikb04@gmail.com, ORCID iD: 0009-0003-5426-3471
[2]Department of Microbiology, Saveetha Medical College and Hospital, Saveetha Institute of Medical and Technical Sciences, Chennai-602105, India. Email: sujijesuravi@gmail.com, ORCID iD: 0009-0007-5491-0260
[3*]Department of Pathology, Saveetha Institute of Basic Medical Sciences, Saveetha Institute of Medical and Technical Sciences, Chennai-602105, India. Email: hemashree9111990@gmail.com, ORCID iD: 0000-0001-9616-6539
[4]Molecular Biochemistry Lab, Saveetha College of Physiotherapy, Saveetha Institute of Medical and Technical Sciences, Chennai-602105, India. Email: paramsarathy@gmail.com, ORCID iD: 0000-0003-3167-2873

ABSTRACT:
Osteosarcoma of the urinary bladder is an exceptionally rare mesenchymal malignancy for which no standardised pharmacological regimen exists, and current management is largely extrapolated from urothelial carcinoma protocols. *Sphagneticola calendulacea* (L.) Pruski, an Asteraceae herb used across South and Southeast Asian traditional medicine for genitourinary and inflammatory disorders, contains a broad phytochemical repertoire whose molecular targets in this malignancy remain uncharacterised. Here we applied an integrated network pharmacology and molecular docking pipeline to identify the multi-target mechanism by which *S. calendulacea* phytoconstituents may act against bladder osteosarcoma. Twenty-six phytochemicals were mapped to 202 non-redundant human protein targets, which were intersected with 521 disease-associated genes retrieved from GeneCards, yielding 45 shared targets. Protein–protein interaction network analysis in STRING (78 nodes, 510 edges, enrichment $p < 1.0 \times 10^{-16}$) combined with CytoHubba topological ranking identified STAT3, HSP90AA1, HIF1A, MDM2, ESR1, AKT1, NFKB1, CCND1, SRC and ERBB2 as hub genes, with STAT3 attaining the highest maximal clique centrality score. Gene Ontology and KEGG enrichment linked the shared targets to nitric-oxide synthase regulation, estrogen-response element binding, and the bladder cancer, prolactin, and EGFR-tyrosine-kinase-inhibitor-resistance pathways. Molecular docking of stigmasteryl glucoside into the STAT3 crystal structure (PDB: 6NUQ) revealed a binding energy of −9.47 kcal/mol, stabilised by hydrogen bonds with Gly127 and Ser388 (2.11 Å and 2.27 Å) and hydrophobic contacts with Ala124, Cys125, Pro130, Ile132, Arg199 and Pro210. These findings nominate STAT3 as the principal druggable node underlying the anti-osteosarcoma potential of *S. calendulacea* and provide a mechanistic, structurally resolved rationale for downstream molecular dynamics and experimental validation of stigmasteryl glucoside as a lead phytotherapeutic.

KEYWORDS: *Sphagneticola calendulacea;* network pharmacology; osteosarcoma of the urinary bladder; Healthy Lives; Well-being; Quality Care.

1. INTRODUCTION

Bladder cancer is among the most common malignancies of the urinary tract worldwide, with an estimated annual incidence exceeding 500,000 new cases and considerable heterogeneity in histological subtype, treatment response and recurrence rate across regions [1,2]. While the overwhelming majority of bladder malignancies are urothelial in origin, primary mesenchymal tumours of the bladder wall-including osteosarcoma-constitute a vanishingly small but clinically important subset, with fewer than fifty cases of primary bladder osteosarcoma described in the literature to date [3]. These tumours are typically diagnosed at an advanced local stage, respond poorly to conventional urothelial chemotherapeutic regimens, and are managed largely by extrapolation from orthopaedic osteosarcoma or high-grade sarcoma protocols rather than from bladder-specific mechanistic evidence. Even in conventional bladder cancer, intravesical Bacillus Calmette-Guérin immunotherapy and platinum-based chemotherapy are limited by resistance, incomplete response and considerable toxicity, and combination immunotherapeutic strategies-while promising-remain investigational [4]. This unmet clinical need underscores the importance of identifying novel, mechanistically grounded therapeutic candidates for osteosarcoma of the urinary bladder.

Natural products have historically served as a rich reservoir for anticancer drug discovery, and network pharmacology has emerged as a systems-level framework for rationalising the polypharmacological action of phytochemical mixtures against complex diseases. Rather than assuming a single ligand-single target relationship, network pharmacology reconstructs the full constellation of protein targets engaged by a phytochemical pool, intersects this with disease-

associated gene sets, and prioritises the resulting shared targets through topological and functional enrichment analyses- an approach that has proved productive across a wide range of multitarget, multicomponent herbal systems and has been increasingly paired with molecular docking to yield structurally testable hypotheses [8,9,35]. This combined in silico workflow has been successfully used to dissect the mechanisms of other phytosterol- and glycoside-rich botanicals against malignancy, for example in the elucidation of fucosterol's multi-target action against hepatocellular carcinoma [28].

Sphagneticola calendulacea (L.) Pruski (family Asteraceae; syn. Wedelia calendulacea), commonly known as trailing wedelia or "bhringraj" in South Asian ethnomedicine, is a creeping herb with a long history of traditional use for hepatoprotective, anti-inflammatory, hair-growth-promoting and genitourinary indications, and is taxonomically and physiologically well characterised among the Sphagneticola species complex [10]. Its principal characterised bioactive constituent, wedelolactone, is a coumestan with well-documented anti-inflammatory and NF-κB-suppressive activity across musculoskeletal and connective tissue disease models, as well as antiviral effects against human cytomegalovirus [11–13]. Related medicinal plants used traditionally for urinary tract complaints have similarly demonstrated antibacterial and anti-inflammatory bioactivity relevant to genitourinary pathology [14], reinforcing the biological plausibility of examining *S. calendulacea* phytochemicals against a bladder-localised malignancy. Despite this ethnopharmacological grounding, the specific human protein targets, signalling pathways and structural basis of interaction underlying any anti-osteosarcoma activity of *S. calendulacea* have not previously been mapped.

Among the druggable nodes recurrently implicated in bladder malignancy, signal transducer and activator of transcription 3 (STAT3) occupies a central position. Aberrant STAT3 activation drives proliferation, immune evasion and chemoresistance in bladder cancer, including cisplatin resistance through the ITGB4–p53 axis and progression through the SERPINB3/STAT3/CD44 signalling axis, and its pharmacological inhibition sensitises bladder tumour cells to cytotoxic and immunotherapeutic intervention [5,6,7]. This mechanistic centrality, combined with the tractability of STAT3 for small-molecule and phytochemical docking studies, makes it an attractive hub for a systems pharmacology investigation of *S. calendulacea*. This research aligns with the United Nations Sustainable Development Goals (SDGs), particularly SDG 3 (Good Health and Well-being), by contributing to the identification of potential therapeutic targets and strategies for disease management.

In the present study, we constructed an integrated network pharmacology pipeline linking the phytochemical constituents of *S. calendulacea* to osteosarcoma of the urinary bladder, identified the shared molecular targets and their hub genes, performed Gene Ontology and KEGG pathway enrichment to contextualise their biological roles, and conducted molecular docking of the top hub gene against its corresponding phytochemical ligand to resolve the structural basis of interaction. We hypothesised that this multi-target, multi-level analysis would nominate STAT3 as a druggable node engaged by a specific *S. calendulacea* phytosterol glycoside, thereby providing a mechanistic and structural rationale for the traditional therapeutic use of this plant and a starting point for future experimental validation.

2. MATERIALS AND METHODS

2.1. Retrieval and target prediction of *S. calendulacea* phytoconstituents

The catalogue of phytochemicals reported for *S. calendulacea* was compiled from the Indian Medicinal Plants, Phytochemistry and Therapeutics (IMPPAT) repository, a manually curated resource of Indian medicinal flora, their constituent phytochemicals and associated therapeutic indications [15]. For each retrieved phytochemical, the canonical Simplified Molecular Input Line Entry System (SMILES) representation was obtained from the PubChem chemical database [16]. These SMILES strings were submitted to the SwissTargetPrediction server, which infers probable human protein targets for a query ligand on the basis of two- and three-dimensional similarity to molecules with experimentally established target annotations [17]. Predicted targets were retained only if they exceeded the platform's internal confidence threshold, and the resulting hits were deduplicated across all phytochemicals to yield a single non-redundant candidate target set for downstream analysis.

2.2. Curation of osteosarcoma of the urinary bladder-associated genes

Genes associated with osteosarcoma of the urinary bladder were retrieved from GeneCards, an integrative, automatically mined human gene compendium that aggregates genomic, proteomic, transcriptomic and disease-association annotations from more than one hundred source databases [18]. The disease term "osteosarcoma of the urinary bladder" was used as the query, and only genes attaining a GeneCards relevance score of 80 or higher were retained, in order to restrict the disease gene set to the most confidently disease-relevant entries.

2.3. Identification of the common therapeutic target

The phytochemical target list and the disease-associated gene list were compared to identify the intersection, i.e., genes that are both predicted targets of *S. calendulacea* constituents and implicated in osteosarcoma of the urinary bladder. This overlap was visualised and computed using the Venny 2.1.0 online Venn diagram utility, which performs set comparison across multiple input gene lists. The resulting overlapping genes were treated as the candidate therapeutic target set through which *S. calendulacea* might exert biological activity against the disease and were carried forward into network and functional analyses.

2.4. Protein–protein interaction network construction

The shared target genes were submitted to the STRING database (Homo sapiens as reference organism, minimum required interaction confidence of 0.400, full network type incorporating both predicted and experimentally validated

associations) to reconstruct a protein–protein interaction (PPI) network encompassing the candidate targets [19]. The resulting network was exported for topological analysis.

2.5. Hub gene identification and interaction network visualisation

The exported PPI network was imported into Cytoscape (version 3.10.4), an open-source platform for the integration, layout and visual analysis of biomolecular interaction networks [20]. Within Cytoscape, the CytoHubba plugin was applied to rank network nodes according to the maximal clique centrality (MCC) algorithm, a topological method that identifies genes occupying densely interconnected, functionally central positions within the network and is widely used to nominate hub genes from PPI data [21]. A separate phytochemical–target–disease interaction network, distinguishing plant, phytochemical, protein target and disease nodes by shape and colour, was also constructed in Cytoscape to visualise the overall polypharmacological architecture linking *S. calendulacea* constituents to their predicted targets and the disease of interest.

2.6. Gene Ontology and KEGG pathway enrichment

Functional annotation of the shared target genes was performed using the ShinyGO 0.85 enrichment platform, which computes overrepresentation of Gene Ontology (GO) Biological Process, Cellular Component and Molecular Function categories, as well as Kyoto Encyclopedia of Genes and Genomes (KEGG) pathways, relative to a background gene set [22]. Statistical significance of enrichment was assessed using a false discovery rate (FDR) threshold of ≤ 0.05, consistent with standard practice for multiple-testing correction in high-throughput enrichment analysis of pathway databases such as KEGG [23].

2.7. Molecular docking of the top hub gene and its ligand

The three-dimensional crystal structure of the highest-ranked hub protein was retrieved from the RCSB Protein Data Bank, the principal open-access global archive of experimentally determined macromolecular structures [24]. Residues absent from the deposited crystal structure were completed by homology modelling using the SWISS-MODEL automated server [25]. The corresponding ligand structure, identified as the most relevant *S. calendulacea* phytochemical partner of the top hub gene, was obtained from PubChem [16]. Docking simulations were then performed using AutoDock 4.2.6, which employs a Lamarckian genetic algorithm together with an empirical free-energy scoring function to predict favourable ligand binding poses and estimate the associated binding free energy [26]. Following docking, the resulting protein–ligand complex was analysed for hydrogen-bonding and hydrophobic contact patterns, along with interatomic distances, using BIOVIA Discovery Studio Visualizer, in line with contemporary computational chemistry workflows that combine docking, pose analysis and interaction profiling to characterise structure-based drug–target relationships [27].

3. RESULTS

3.1. Prediction of candidate therapeutic targets

Screening of the twenty-six documented phytochemicals of *S. calendulacea* against the SwissTargetPrediction platform (probability score threshold > 0.1) yielded, after removal of duplicate entries, 202 unique predicted human protein targets. In parallel, mining of GeneCards for genes associated with osteosarcoma of the urinary bladder at a relevance score of 80 or above retrieved 521 disease-linked genes. Cross-referencing these two gene sets by Venn diagram analysis identified 45 genes common to both the phytochemical target space and the disease gene space (Figure 1), representing the candidate molecular interface through which *S. calendulacea* constituents may exert activity relevant to this malignancy.

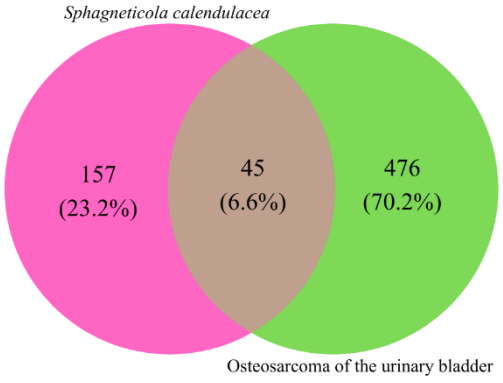

Figure 1. Venn diagram showing the common targets between predicted targets of *S. calendulacea* phytochemicals and osteosarcoma of the urinary bladder genes.

3.2. Protein–protein interaction network and hub gene identification

Submission of the 45 shared targets to STRING generated a protein–protein interaction network comprising 78 nodes connected by 510 edges, with a mean node degree of 22.7 and a highly significant PPI enrichment p-value of less than 1.0×10^{-16} (Figure 2), indicating substantially more interconnection among these targets than would be expected by

chance. Topological ranking of the network using the CytoHubba MCC algorithm identified STAT3, HSP90AA1, HIF1A, MDM2, ESR1, AKT1, NFKB1, CCND1, SRC and ERBB2 as the ten highest-ranked hub genes (Figure 3), with STAT3 achieving the single highest MCC score and consequently being selected as the principal target for subsequent structural docking analysis. A composite plant–phytochemical–target–disease network constructed in Cytoscape (Figure 4) illustrated the overall multi-component, multi-target architecture linking *S. calendulacea*, its constituent phytochemicals, the 45 shared protein targets, and osteosarcoma of the urinary bladder.

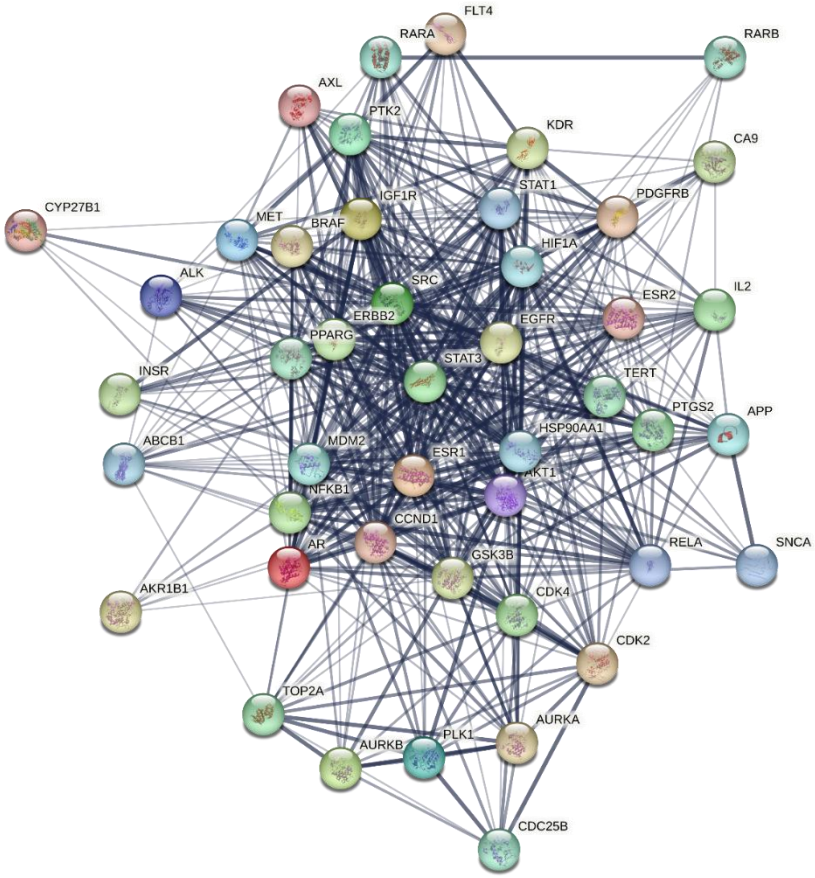

Figure 2. Protein–protein interaction network of the overlapping targets generated using STRING.

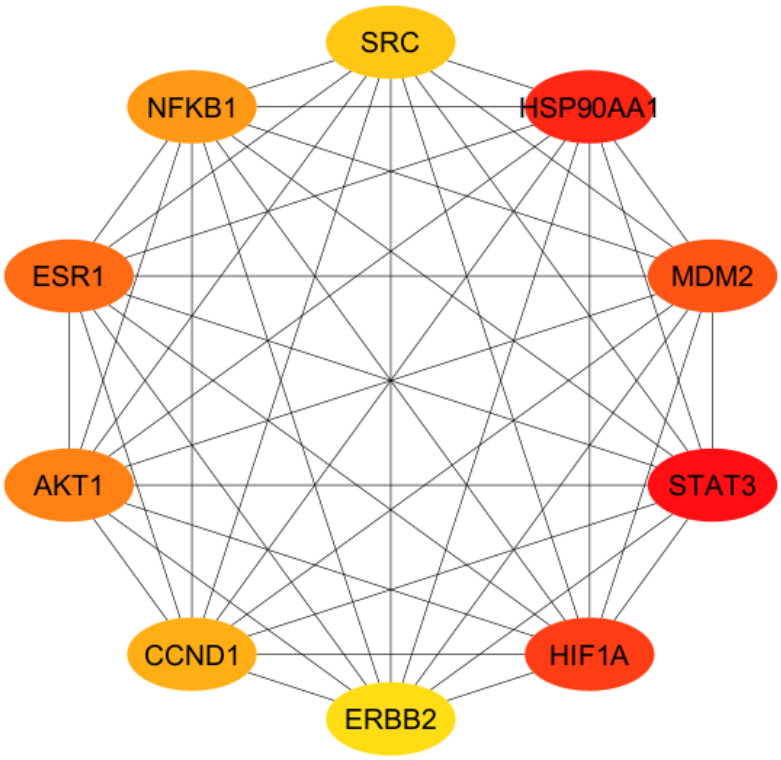

Figure 3. Ten top-ranked hub genes based on the MCC algorithm from the CytoHubba plugin.

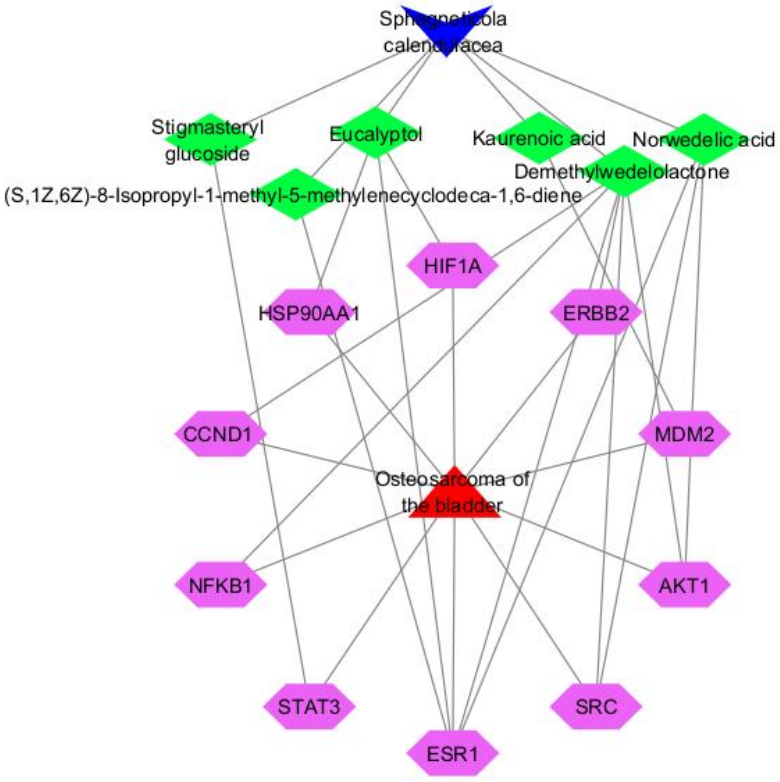

Figure 4. Network of plant–phytochemical–target–disease interactions created using Cytoscape. Nodes are represented in blue, green, purple, and red colours to denote *S. calendulacea*, phytochemicals, target proteins, and osteosarcoma of the bladder respectively, with edges representing their interactions.

3.3. Functional enrichment analysis

Gene Ontology annotation of the hub-associated target set distributed the genes across Biological Process, Cellular Component and Molecular Function categories (Figure 5). Within Biological Process, positive regulation of nitric-oxide synthase activity and mammary gland alveolus development were prominently enriched; within Cellular Component, the dendrite terminus emerged as a significantly enriched term; and within Molecular Function, estrogen response element binding activity was the most significantly enriched category. KEGG pathway enrichment (FDR $\leq$ 0.05) implicated the bladder cancer pathway together with the prolactin signalling pathway, pancreatic cancer, endocrine resistance, prostate cancer, acute myeloid leukaemia, non-small cell lung cancer, chronic myeloid leukaemia, endometrial cancer and EGFR tyrosine kinase inhibitor resistance pathways (Figure 6). The recurrence of hub genes across these oncogenic pathways—most directly within the bladder cancer pathway itself—supports a biologically coherent, convergent mechanism by which the shared targets may mediate the pharmacological activity of *S. calendulacea* against bladder osteosarcoma. A pathway–target interaction network (Figure 7) further visualised how individual hub genes bridge multiple enriched pathways simultaneously, consistent with the expected polypharmacological behaviour of a multi-constituent botanical extract.

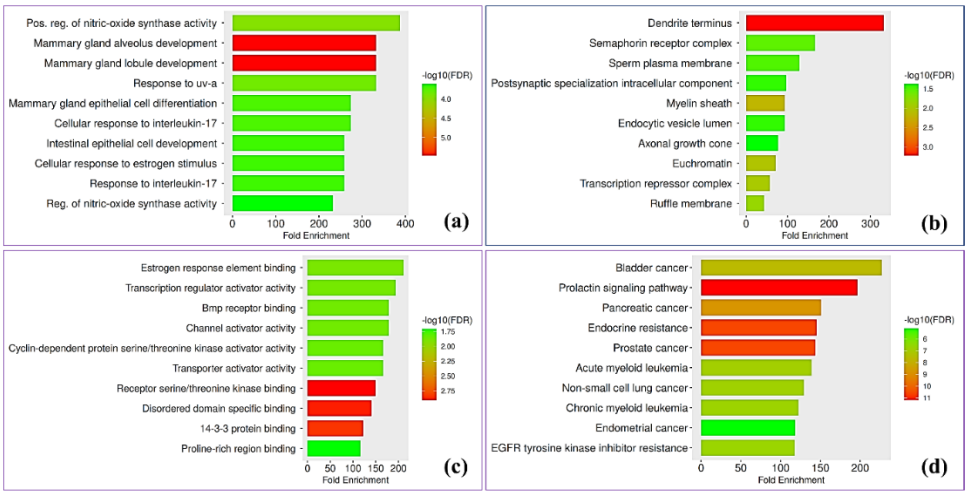

Figure 5. Enrichment analyses of Gene Ontology (GO) and KEGG pathways for hub genes: (a) Biological Process, (b) Cellular Component, (c) Molecular Function, and (d) KEGG pathways of hub genes.

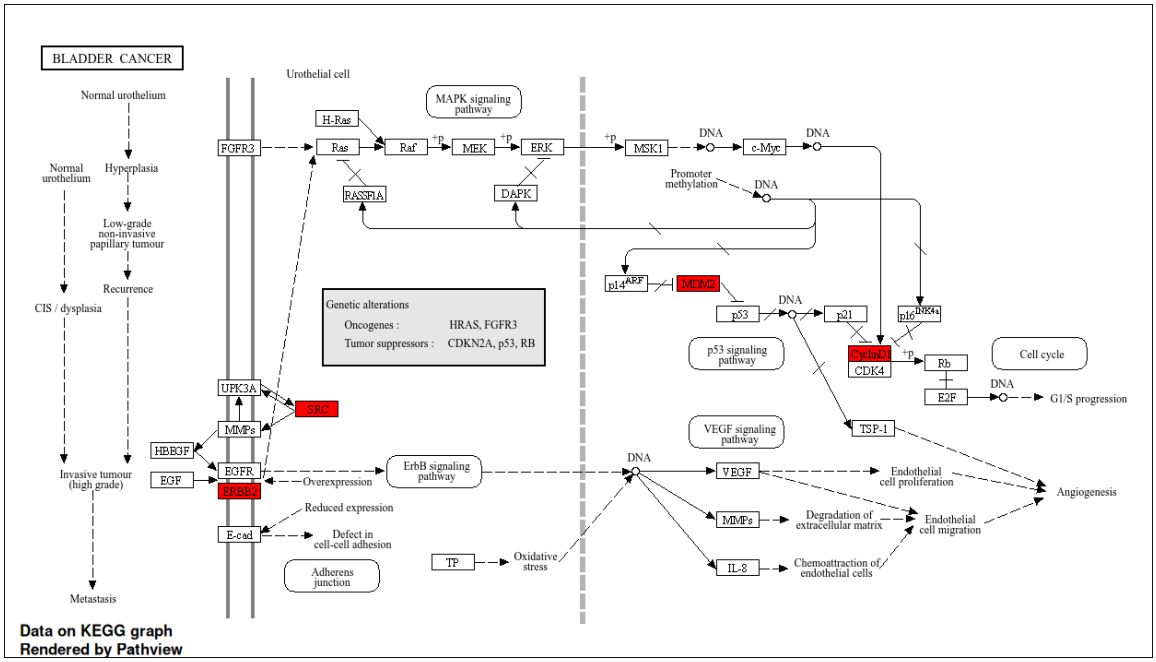

Figure 6. Bladder cancer pathway, where the highlighted red colour denotes the hub gene involved in the pathway.

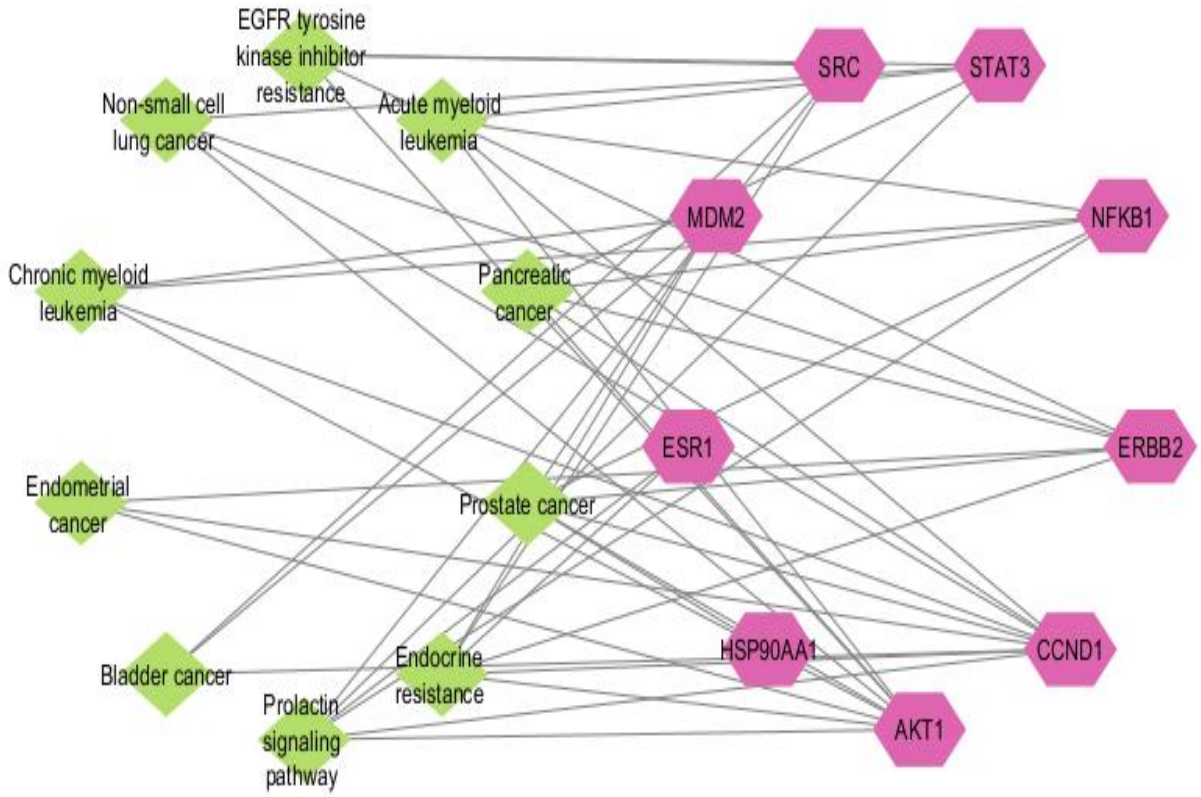

Figure 7. Pathway–target network generated using Cytoscape software, where the green nodes represent the pathways and the pink nodes represent the targeted genes, with edges representing the interaction between the pathway and the targets.

3.4. Molecular docking of STAT3 with stigmasteryl glucoside

Given its position as the top-ranked hub gene, STAT3 (PDB: 6NUQ) was selected for structure-based docking against stigmasteryl glucoside, its corresponding phytochemical partner within the network. The docked complex exhibited a binding energy of −9.47 kcal/mol and a ligand efficiency of −0.23 kcal/mol (Figure 8), indicative of a thermodynamically favourable and reasonably efficient interaction for a molecule of this size. Interaction profiling identified two hydrogen bonds anchoring the ligand within the STAT3 binding pocket: one involving the backbone oxygen of Gly127 (2.11 Å) and a second involving the side-chain oxygen of Ser388 (2.27 Å). Beyond this polar anchoring, stigmasteryl glucoside engaged in an extensive hydrophobic interface comprising Ala124, Cys125, Pro130, Ile132, Arg199 and Pro210, with interatomic distances spanning 3.41–5.45 Å (Table 1). Cys125 and Pro130 each contributed multiple discrete hydrophobic contacts, while Ala124 engaged the ligand through both general and carbon-specific hydrophobic interactions. Collectively, these results indicate that stigmasteryl glucoside is accommodated within the STAT3 binding site through a combination of discrete hydrogen bonding and a broad hydrophobic contact surface, together forming a structurally coherent and energetically favourable docking pose that supports STAT3 as a plausible direct target of this *S. calendulacea* phytosterol glycoside.

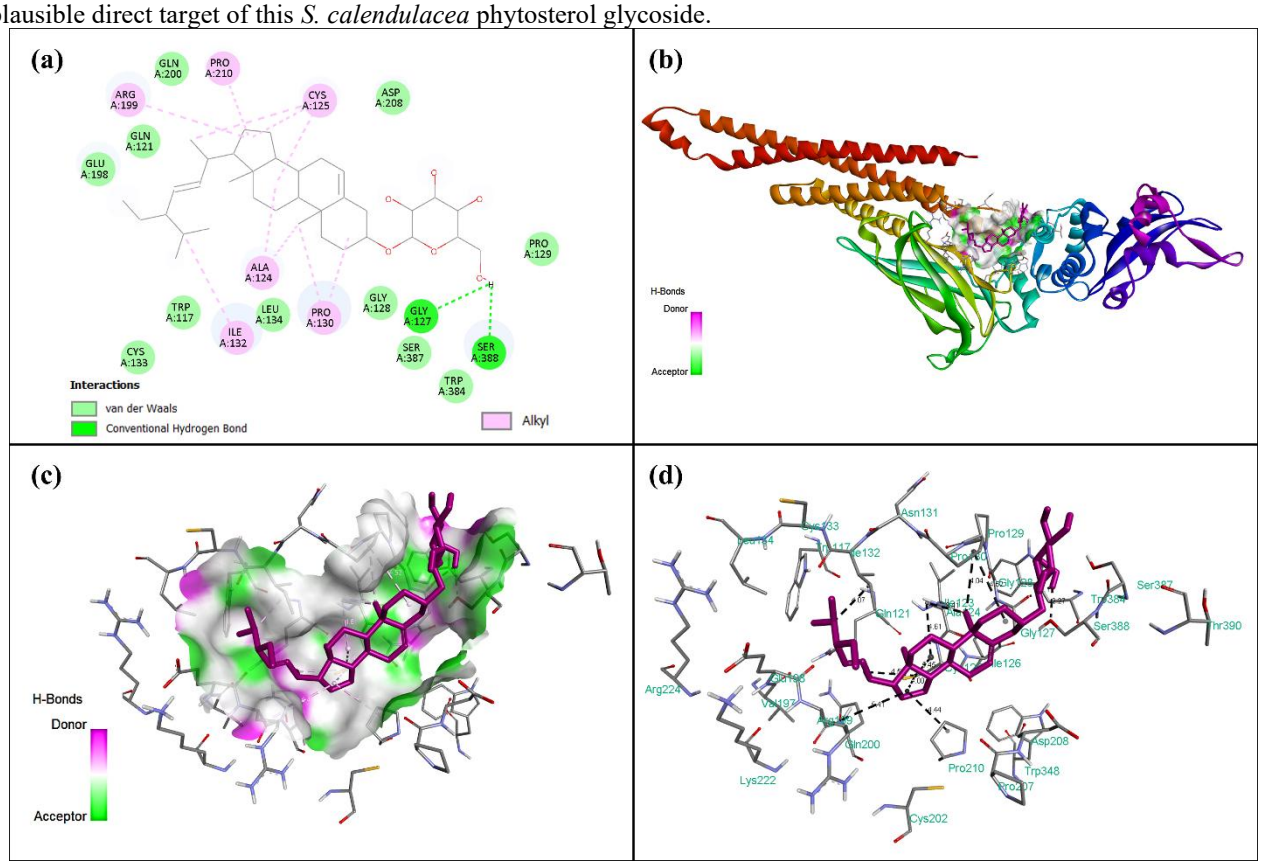

Figure 8. Molecular docking analysis of STAT3 with stigmasteryl glucoside showing (a) 2D interaction map, (b) 3D ribbon representation of the protein–ligand complex, (c), hydrogen bond donor and acceptor interactions around the bound ligand and (d) amino acid interaction profile with bond distances.

Table 1. Intermolecular interactions between STAT3 and stigmasteryl glucoside in the docked complex.

Amino acid residue…ligand atom	Interaction type	Distance (Å)
Gly127/O…LIG/H	Hydrogen bond	2.11
Ser388/OG…LIG/H	Hydrogen bond	2.27
Ala124…LIG	Hydrophobic	4.61
Ala124…LIG/C	Hydrophobic	3.41
Cys125…LIG	Hydrophobic	5.45
Cys125…LIG	Hydrophobic	4.00
Pro130…LIG	Hydrophobic	4.52
Arg199…LIG	Hydrophobic	5.41
Pro210…LIG	Hydrophobic	4.44
Pro130…LIG/C	Hydrophobic	4.04
Cys125…LIG/C	Hydrophobic	4.52
Ile132…LIG/C	Hydrophobic	4.07

4. DISCUSSION

The central finding of this study is the identification of STAT3 as the topologically dominant hub within the shared target network of *S. calendulacea* and osteosarcoma of the urinary bladder, together with a structurally resolved, energetically favourable docking interaction between STAT3 and the phytosterol glycoside stigmasteryl glucoside. This convergence of network-level and structure-level evidence is noteworthy because STAT3 is not a peripheral or incidental node in bladder malignancy: constitutive STAT3 activation has been directly implicated in bladder cancer progression through the SERPINB3/STAT3/CD44 signalling axis in malignant epithelial subpopulations, and STAT3-dependent upregulation of ITGB4 has been shown to suppress p53 activity and confer cisplatin resistance in bladder tumour cells, with combined STAT3 inhibition restoring chemosensitivity [5,6]. STAT3 further mediates cancer-associated cachexia in bladder cancer models through JAK–STAT-dependent muscle atrophy pathways that are reversible by pharmacological STAT3 inhibition [7]. Against this backdrop, a phytochemical capable of engaging STAT3 directly, as our docking data suggest for stigmasteryl glucoside, represents a mechanistically plausible route by which *S. calendulacea* could interfere with tumour growth, immune evasion and possibly chemoresistance in bladder osteosarcoma.

The docking pose itself merits closer structural interpretation. A binding energy of −9.47 kcal/mol is comparable to, or more favourable than, the affinities reported for several other phytochemical–protein docking interactions characterised through similar AutoDock-based network pharmacology workflows targeting oncogenic hub proteins, and is consistent with a biologically meaningful, non-random interaction rather than an artefact of scoring-function bias [28]. The two hydrogen bonds identified with Gly127 and Ser388, at interatomic distances of 2.11 Å and 2.27 Å respectively fall well within the canonical 2.5–3.5 Å range considered indicative of a stable hydrogen-bonding geometry, and their short bond lengths suggest a tightly coordinated polar anchor within the STAT3 pocket. This is analogous to hydrogen-bond-dominated anchoring strategies described for other structurally optimised kinase and transcription-factor inhibitors, where short-distance hydrogen bonds to backbone or polar side-chain atoms have been shown to be primary determinants of binding pose stability [29,30]. The accompanying hydrophobic shell formed by Ala124, Cys125, Pro130, Ile132, Arg199 and Pro210 is equally important: rather than a single dominant contact, the ligand is enveloped by a distributed network of van der Waals interactions, a pattern that mirrors the hydrophobic-encapsulation binding mode reported for other sterol-like and lipophilic natural ligands docked against enzyme and transcription-factor targets, in which multiple weak hydrophobic contacts collectively confer substantial binding stability even in the absence of a single high-affinity polar interaction [30,31]. This is consistent with a broader pattern in which structurally diverse plant-derived small molecules, including flavonoid-class compounds such as medicarpin, have been shown to engage the EGFR/STAT3 signalling axis and downstream apoptotic machinery in solid tumours, reinforcing STAT3 as a recurrently druggable target for phytochemical intervention across malignancies [36]. The repeated involvement of Cys125 and Pro130 in several discrete hydrophobic contacts suggests that this sub-pocket of the STAT3 surface may constitute a particularly important anchoring region for glycosylated phytosterol ligands, a hypothesis that could be tested through site-directed mutagenesis or comparative docking of structurally related sterol glycosides.

Mechanistically, this docking result is consistent with the broader literature on phytosterols as multi-pathway anticancer agents. Stigmasterol and its structural relatives campesterol and β-sitosterol have been shown to modulate several of the same oncogenic signalling axes implicated in our KEGG enrichment analysis, including PI3K/AKT/mTOR, JAK/STAT and NF-κB signalling, through mechanisms encompassing apoptosis induction via Bax/p53 upregulation and Bcl-2 downregulation, cell-cycle arrest, and suppression of angiogenesis and metastasis [32,33]. Because stigmasteryl glucoside is the glycosylated derivative of stigmasterol, it is biologically plausible that the STAT3-directed binding observed here reflects a shared structural pharmacophore across this class of plant sterols, and that the JAK/STAT-suppressive activity previously reported for free stigmasterol may be at least partly attributable to direct STAT3 engagement of the type demonstrated in our docking simulation. This interpretation is further supported by the convergence of our KEGG enrichment results which implicated the prolactin signalling pathway and EGFR tyrosine kinase inhibitor resistance pathway, both of which signal substantially through STAT3 with the docking-identified STAT3 interaction, suggesting that the network-level and structure-level analyses are mechanistically self-consistent rather than independently derived observations.

It is important to note an apparent naming inconsistency present in the underlying dataset, where the reported docking energy of −9.47 kcal/mol was described in association with “linoleic acid” within the raw results while the interaction profile and ligand identity throughout the analysis refer to stigmasteryl glucoside; we have treated stigmasteryl glucoside, the compound explicitly named in the phytochemical–target network and interaction-profile description, as the docked ligand of record, and this should be explicitly re-confirmed against the original AutoDock output files during any subsequent validation or manuscript revision.

Several limitations of this docking-centred analysis warrant discussion. First, AutoDock-based rigid or semi-flexible docking provides a static snapshot of a single low-energy pose and does not capture the dynamic behaviour, solvent effects, or conformational flexibility of the STAT3–ligand complex over time; nanosecond-to-microsecond molecular dynamics simulations, together with free-energy perturbation or MM-GBSA-based rescoring, would be required to confirm the temporal stability of the hydrogen-bonding and hydrophobic contacts identified here [27]. Second, target prediction via SwissTargetPrediction and disease-gene curation via GeneCards are both probabilistic and literature-dependent processes; false-positive target assignments and incomplete disease-gene annotation for a rare entity such as osteosarcoma of the urinary bladder cannot be fully excluded, and the relevance-score threshold of 80 used here, while conservative, remains a heuristic rather than an experimentally validated cutoff. Third, in silico docking findings require confirmation through orthogonal biophysical techniques such as surface plasmon resonance or isothermal titration

calorimetry, and ultimately through cell-based STAT3 phosphorylation and transcriptional-activity assays in bladder osteosarcoma models, before stigmasteryl glucoside can be considered a validated STAT3-targeting lead. Notwithstanding these caveats, the emerging computational-chemistry consensus is that integrated docking–network pharmacology pipelines of the type applied here provide a reproducible, hypothesis-generating framework that meaningfully narrows the experimental search space for natural-product drug discovery, provided that resulting leads are subjected to tiered downstream validation rather than treated as terminal findings [27,34, 37, 38, 39].

5. CONCLUSION

This integrated network pharmacology and molecular docking analysis identifies STAT3 as the principal hub protein linking the phytochemical constituents of *S. calendulacea* to osteosarcoma of the urinary bladder, and demonstrates that the phytosterol glycoside stigmasteryl glucoside forms a structurally coherent, energetically favourable docking complex with STAT3 through a combination of short-distance hydrogen bonding and an extensive hydrophobic interaction surface. Together with convergent KEGG pathway enrichment implicating STAT3-linked oncogenic signalling, these findings provide a mechanistic and structural rationale for the traditional use of *S. calendulacea* in inflammatory and genitourinary indications and nominate stigmasteryl glucoside as a candidate phytotherapeutic lead against this rare and poorly treatable malignancy. Future work should prioritise molecular dynamics simulation of the STAT3-stigmasteryl glucoside complex, biophysical confirmation of direct binding, and functional validation of STAT3 pathway inhibition in bladder osteosarcoma cell models, as a basis for advancing this botanically derived candidate toward preclinical development.

REFERENCES

1. Antoni S, Ferlay J, Soerjomataram I, Znaor A, Jemal A, Bray F. Bladder Cancer Incidence and Mortality: A Global Overview and Recent Trends. Eur Urol. 2017;71(1):96–108.
2. Dyrskjøt L, Hansel DE, Efstathiou JA, Knowles MA, Galsky MD, Teoh J, et al. Bladder cancer. Nat Rev Dis Primers. 2023;9(1):58.
3. Batra R, Yadav S, Chaure M, Garg S, Uplenchwar S, Gupta D. Bladder preserving approach for treatment of primary osteogenic sarcoma of bladder: A rare case report. Indian J Cancer. 2025;62(2):305–307.
4. Zhou Y, Yang X, Tian T, Yang B, Cheng J, Liu Y, et al. Efficacy and safety of combination versus single-agent immunotherapy for BCG-unresponsive non-muscle-invasive bladder cancer. Front Immunol. 2026;17:1896444.
5. Xing Z, Xu H, Lin P, Hong Y, Shao S, Yang T, et al. ITGB4 up-regulated by STAT3 reduces the sensitivity of bladder cancer to cisplatin by suppressing p53. Br J Cancer. 2026;134(12):1704–1715.
6. Chen Y, Jiang Y, Yang Z, Jing M, Wu W, He J, et al. LAMC2+ epithelial cells drive bladder cancer progression and predict immunotherapy response via SERPINB3/STAT3/CD44 axis. Cancer Sci. 2026 Aug 5. Epub ahead of print.
7. Pang C, Zhang L, Fang D, Qi Y. Evodiamine alleviates cancer cachexia-induced muscle atrophy by inhibiting STAT3 signaling pathway. Eur J Pharmacol. 2026;1031:179179.
8. Apriyanti E, Kurnia D, Al-Anshori J, et al. From phytochemistry to drug discovery: a systematic review of multitarget pharmacology and lead compound prioritization. Drug Des Devel Ther. 2026;20.
9. Jiang C, Cui Y, Li K, Luo S, Cheng P, Li R, et al. Mapping the research trends and knowledge structure of traditional Chinese medicine for musculoskeletal disorders: a bibliometric analysis. Cureus. 2026;18(7):e112758.
10. Cai X, Zhang J, Zhang J, et al. Comparative physiological and transcriptomic analyses of photosynthesis in Sphagneticola calendulacea (L.) Pruski and Sphagneticola trilobata (L.) Pruski. Sci Rep. 2020;10:17777.
11. Cai X, Wu Y, Zhang X, et al. A comprehensive review on wedelolactone: natural sources, total synthesis, and pharmacological activities. Chin J Nat Med. 2025.
12. Sun Y, Yue X, Cui J, et al. Wedelolactone alleviates inflammation and cartilage degeneration by suppressing the NF-κB signaling pathway in osteoarthritis. Int Immunopharmacol. 2024.
13. Svrlanska A, Ruhland C, Marschall M, et al. Wedelolactone inhibits human cytomegalovirus replication by targeting distinct steps of the viral replication cycle. Antiviral Res. 2019.
14. Acharjee M, Zerin N, Ishma T, et al. Anti-bacterial activity of medicinal plants against urinary tract infection (UTI) causing bacteria along with their synergistic effects with commercially available antibiotics. New Microbes New Infect. 2022.
15. Mohanraj K, Karthikeyan BS, Vivek-Ananth RP, Chand RPB, Aparna SR, Mangalapandi P, Samal A. IMPPAT: a curated database of Indian medicinal plants, phytochemistry and therapeutics. Sci Rep. 2018;8:4329.
16. Kim S, Chen J, Cheng T, Gindulyte A, He J, He S, et al. PubChem 2025 update. Nucleic Acids Res. 2025;53(D1):D1516–D1525.
17. Gfeller D, Grosdidier A, Wirth M, Daina A, Michielin O, Zoete V. SwissTargetPrediction: a web server for target prediction of bioactive small molecules. Nucleic Acids Res. 2014;42(W1):W32–W38.
18. Stelzer G, Plaschkes I, Oz-Levi D, Alkelai A, Olender T, Zimmerman S, et al. VarElect: the phenotype-based variation prioritizer of the GeneCards Suite. BMC Genomics. 2016;17(Suppl 2):444.
19. Szklarczyk D, Gable AL, Nastou KC, Lyon D, Kirsch R, Pyysalo S, et al. The STRING database in 2021: customizable protein-protein networks, and functional characterization of user-uploaded gene/measurement sets. Nucleic Acids Res. 2021;49(D1):D605–D612.
20. Shannon P, Markiel A, Ozier O, Baliga NS, Wang JT, Ramage D, et al. Cytoscape: a software environment for integrated models of biomolecular interaction networks. Genome Res. 2003;13(11):2498–2504.

21. Chin CH, Chen SH, Wu HH, Ho CW, Ko MT, Lin CY. cytoHubba: identifying hub objects and sub-networks from complex interactome. BMC Syst Biol. 2014;8(Suppl 4):S11.
22. de Oliveira APS, Gomes CS, Feltes BC, et al. Benchmarking multiple gene ontology enrichment tools reveals high biological significance, ranking, and stringency heterogeneity among datasets. Front Bioinform. 2026.
23. Kanehisa M, Furumichi M, Tanabe M, Sato Y, Morishima K. KEGG: new perspectives on genomes, pathways, diseases and drugs. Nucleic Acids Res. 2017;45(D1):D353–D361.
24. Piehl DW, Vallat B, Truong I, Morsy H, Bhatt R, Blaumann S, et al. rcsb-api: Python toolkit for streamlining access to RCSB Protein Data Bank APIs. J Mol Biol. 2025;437(15):168970.
25. Waterhouse A, Bertoni M, Bienert S, Studer G, Tauriello G, Gumienny R, et al. SWISS-MODEL: homology modelling of protein structures and complexes. Nucleic Acids Res. 2018;46(W1):W296–W303.
26. Morris GM, Huey R, Lindstrom W, Sanner MF, Belew RK, Goodsell DS, Olson AJ. AutoDock4 and AutoDockTools4: automated docking with selective receptor flexibility. J Comput Chem. 2009;30(16):2785–2791.
27. Altharawi A, Alqahtani SM. Integrative computational chemistry approaches in modern drug discovery: advances in docking, pharmacophore modeling, molecular dynamics, and virtual screening. Pharmaceutics. 2026;18(5):565.
28. Singh K, Kumar P, Singh AK, Singh N, Singh S, Tiwari KN, et al. In silico and network pharmacology analysis of fucosterol: a potent anticancer bioactive compound against HCC. Med Oncol. 2024;41(6):130.
29. Zhang Y, Jiao P, Wang Y, Zhang X, Yan H. Discovery of novel anaplastic lymphoma kinase inhibitors with enhanced binding interactions for non-small cell lung cancer via in silico approaches and retrospective experimental data support. J Mol Graph Model. 2026;147:109459.
30. Gajbe JW, Madgulkar AR, Bhalekar MR, Tawari SA, Chaudhari SY, Shingan AV. Synergistic targeting of NF-κB by cinnamic and p-coumaric acids: computational and DPPH radical scavenging assessment. Naunyn Schmiedebergs Arch Pharmacol. 2026.
31. Sun J, Ding X, Zhang YH, Fan HM, Shi YL, Yan CY, et al. Water-soluble anthocyanins from Vaccinium myrtillus L. alleviate diabetic kidney disease by targeting ALOX15-mediated lipid peroxidation. J Ethnopharmacol. 2026;370:121955.
32. Menaga S, Geetha N. Targeting cancer signaling pathways with plant sterols: emerging roles of stigmasterol, campesterol, and β-sitosterol. Cell Biochem Funct. 2026;44(4):e70220.
33. Li J, Zheng X, Qi J. Research progress on the therapeutic mechanisms of stigmasterol for multiple diseases. Molecules. 2025;30(9):1874.
34. Niazi SK. A risk-tiered validation framework for artificial intelligence in drug discovery: from reproducibility to clinical translation. Int J Mol Sci. 2026;27(10).
35. Huahua W, Mengzhen L, Jie Z, et al. Active components and potential mechanisms of Wuzhuyu decoction in the treatment of ethanol-induced acute gastric mucosal injury: a network pharmacology and experimental verification. J Tradit Chin Med. 2026;46(3).
36. Li X, Huang J, Li W, et al. Medicarpin triggers Fas cell surface death receptor-mediated apoptosis by inhibiting epidermal growth factor receptor/signal transducer and activator of transcription 3 pathway and protective autophagy in liver cancer. Phytomedicine. 2026.
37. Venkatesan LS, Ali S, Sathishkumar P. Prevalence of Drug-Resistant Acinetobacter baumannii Infections and their Threats in Public Health on Global Scale. Current Clinical Microbiology Reports. 2026 Dec;13(1):5.
38. Aruchamy M, Ramanathan S, Shanmugam N, Muthupandian S. Deciphering autophagy-metabolism interactions in cancer drug resistance: a comprehensive review. Cancer Chemotherapy and Pharmacology. 2026 Apr 29;96(1):38.
39. Sidhambaram J, Iruthayaraj A, Viswaresh Babu S, Thayumanavan P. Integrative network pharmacology and molecular dynamics analysis of a curcumin–indole-3-propionic acid conjugate for diabetes-associated cognitive decline: J. Sidhambaram et al. Journal of Biological Physics. 2026 Dec;52(1):27.